Photoluminescence in silicon powder grown by plasma-enhanced chemical-vapor deposition: Evidence of a multistep-multiphoton excitation process

P. Roura, J. Costa, G. Sardin, J. R. Morante, and E. Bertran
Departament de Física Aplicada i Electrònica, Facultat de Física, Universitat de Barcelona, Avenida Diagonal 647, Barcelona E-08028, Catalonia, Spain
(Received 13 June 1994)

The dynamics of the infrared photoluminescence (PL) in silicon powder grown by plasma-enhanced chemical-vapor deposition (PECVD) of silane is reported. A nonlinear dependence of PL intensity on laser power of the form $I \propto P^n$ with n as high as 7 has been found, indicating a multistep-multiphoton excitation process. To confirm this hypothesis a very detailed theoretical and experimental analysis has been performed. As a result, the lifetimes of several levels in the excitation chain have been determined, as well as the optical cross section (σ). For the slowest level $\sigma = 3 \times 10^{-18}$ cm^2 and the lifetime is as long as 400 ms. As the energy of the emitted photon is smaller than that of the excitation photon, a model involving a considerable nonradiative energy relaxation, together with a tunnel effect is proposed.

I. INTRODUCTION

The formation of silicon nanopowder involved in plasma-enhanced chemical-vapor-deposition (PECVD) processes has stimulated many reports.[1,2] Efforts have been made to determine its effect on the growing film and to monitor the reaction conditions in order to enhance the powder production. This material is expected to be a good precursor for sintering ceramics and for catalytic surfaces.

Similar to other nanostructured silicon materials, such as porous silicon[3] and silicon nanocristallites,[4] silicon nanopowder formed in PECVD shows an intense photoluminescence (PL) emission. It has been observed in the powder suspended in the plasma[5] and by *ex situ* analysis.[6] However, its properties reveal that this PL is qualitatively different.[6] (i) Its intensity decreases dramatically as the gas pressure inside the cryostat (where the samples were mounted) increases, making it unmeasurable at atmospheric pressure. This evolution is exponential, $I_{PL} = I_0 \exp(-P/P_0)$, where $P_0 \approx 1.5$ Pa, indicating that it is related to a quite simple microscopic mechanism. (ii) The dependence on laser power is highly supralinear ($I_{PL} \propto \Phi^r, r = 4-7$). (iii) Long lifetimes, of hundreds of ms, are measured.

We present an extensive study of the PL dynamics of silicon powder, showing that it follows what we call a multistep-multiphoton excitation process.

This paper is organized as follows. After a brief description of material structure and experimental equipment (Sec. II), a description of general PL results is given in Sec. III. In Sec. IV, these results are compared with several excitation mechanisms described in the literature. It is concluded that only the multistep-multiphoton model can account for all experimental features. Then, in Sec. V we develop a theoretical analysis of the dynamic behavior expected for an ideal multistep-multiphoton excitation process. From this analysis we establish the relevant features to be observed experimentally. It is shown that, from the dependence of PL intensity on laser power and from the beginning of the excitation transient, the number of steps involved in the process can be deduced. In addition, the lifetimes related to the luminescent as well as to intermediate nonluminescent levels can be obtained by analyzing the excitation and deexcitation transients. The measurements are reported in Sec. VI following the same scheme as in the theoretical analysis. This structure highlights the very good agreement between theory and experiment. In this section a method is developed to obtain the distribution of time constants that contribute to a nonexponential transient. Finally, we summarize the results, and a discussion is included where several refinements are introduced in the model.

II. EXPERIMENT

The procedure for obtaining silicon powder by PECVD is described in Ref. 6. Its structural characteristics have been analyzed by a number of techniques (micro-Raman and infrared spectroscopies, electron and x-ray diffraction, electron microscopy, and others) and the results are reported in previous works.[6-9] Essentially, it is constituted by amorphous silicon particles with diameters ranging from 10 to 200 nm. These particles are highly hydrogenated (about 30% hydrogen content) with a predominance of SiH_2 groups over SiH bonds. Once exposed to the atmosphere, rapid spontaneous oxidation occurs. Macroscopically, PECVD silicon powder is reddish with a very poor mechanical consistency and low density (about 10 mg/cm^3).

The PL was excited by the 488-nm line of an Ar laser which was focused on a 4-mm^2 spot on the sample surface. The incident laser power ranged from 1 to 20 mW. To cut the laser beam a mechanical shutter was used whose commutation time was 2 ms. The PL spectra were analyzed by a 0.5-m monochromator and detected with an InAs photodiode cooled to 77 K. The spectra were corrected by the system transfer function.

Two spectral regions were analyzed in detail. The PL transients with emission energy at 1.55 eV were measured

with a GaAs photomultiplier cooled to −30°C. The emission between 0.4 and 0.7 eV was integrated with the InAs detector by replacing the monochromator diffraction grating with a mirror, and the limits were determined by optical filters.

Samples were mounted inside a closed-circuit helium cryostat, in which the gas pressure was held at 10^{-2} Pa. All PL measurements described were carried out at room temperature and under vacuum.

III. GENERAL RESULTS

In this section, we will describe the general results that have led us to analyze in detail the multistep-multiphoton excitation process. In view of this theoretical analysis, more experiments are proposed which are reported in Sec. VI.

The PL spectrum is a structureless broad band covering the near-infrared region (Fig. 1). It begins just below the excitation energy (2.5 eV) and continues beyond the detection limit (0.4 eV). Its slope changes with excitation power. In Fig. 1 we can see that the relative intensity at higher photon energies increases with laser power.

The dependence of PL intensity on excitation power is very nonlinear. In Fig. 2, it is shown that it follows the supralinear dependence

$$I_{PL} \propto \phi^r , \tag{1}$$

where r depends on the spectral region. At 1.5 eV the slope in the log-log plot evolves from 7 to 3.5 as the excitation power increases, whereas it is comprised between 3.3 and 1.8 when we integrate the PL in the 0.4–0.7-eV region.

PL intensity was recorded during and after a 2-s laser pulse (Fig. 3). When the laser turned on, the intensity began to grow with zero slope (inset of Fig. 3), and the steady state was finally reached with an exponential evolution described by a time constant as large as 400 ms. After turning the laser off, the PL decay was quasiexponential with a lifetime of about 20 ms.

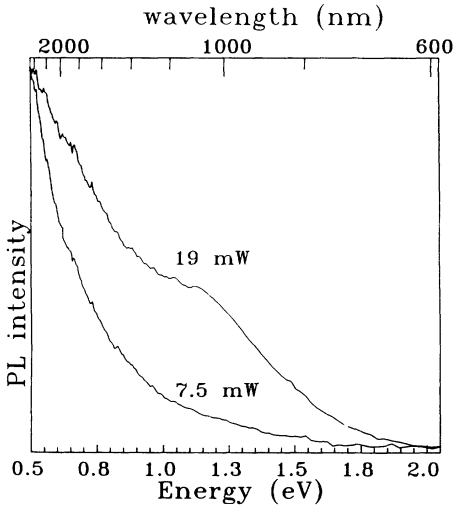

FIG. 1. PL spectra measured at room temperature.

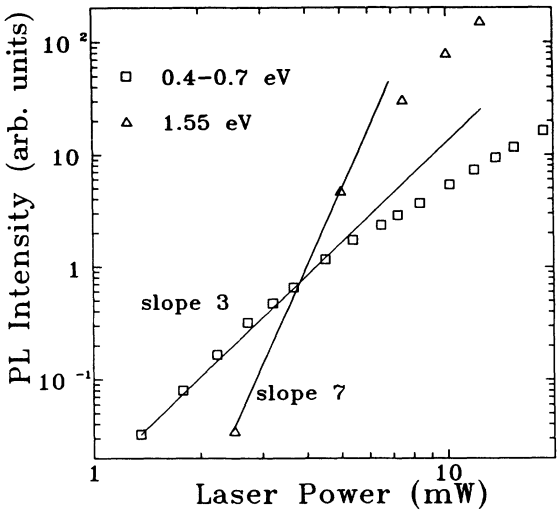

FIG. 2. Dependence of PL intensity at steady-state conditions on laser power.

IV. ANALYSIS

The energy-level structure giving rise to this PL behavior cannot be described by a simple two-level model. A more elaborate model has to be built taking into account three main features.

(a) The nonlinear dependence of the PL intensity (I_{PL}) with excitation photon flux (Φ) which is approximately given by Eq. (1), where r can be as large as 7 (Fig. 2).

(b) The zero slope at the beginning of the excitation transient (inset of Fig. 3).

(c) The fact that the excitation time constant is longer than the PL decay lifetime (Fig. 3).

Many materials have been reported in literature which exhibit similar behavior. Their PL properties can be understood mainly in terms of three processes: the energy transfer process, one-step multiphoton excitation, and multistep-multiphoton excitation.

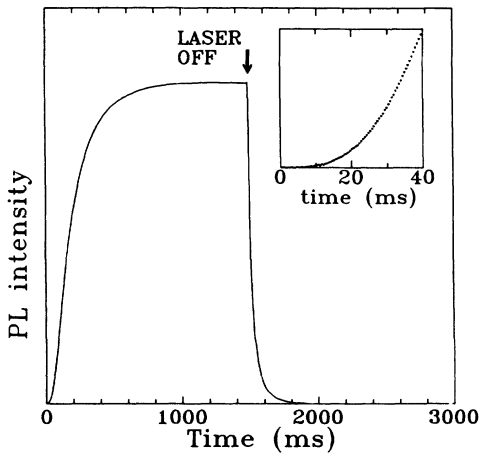

FIG. 3. Excitation and decay transients when a laser pulse 2-s long is applied. In the inset note the zero slope at the beginning of the excitation.

(a) In an energy-transfer process, the excitation transient begins with zero slope. The absorption of one photon is needed to promote the system to an intermediate state. Then the excitation until the luminescent state is achieved with an internal energy transfer.[10–12] Occasionally, this kind of process could give an excitation time constant longer than the deexcitation one. However, at steady-state conditions, the PL intensity would increase linearly with laser power.

(b) In one-step multiphoton excitation, the excited state is reached directly by simultaneous absorption of several photons.[13] The exponent r in Eq. (1) is indeed the number of photons involved in the transition (usually $r=2$). This kind of process usually requires a very high photon density only achieved with pulsed lasers. However, the slope at the beginning of the transient would have a finite value.

(c) The multistep-multiphoton excitation is similar to the previous process. However, in this case, with the absorption of one photon the system reaches an intermediate state. A subsequent absorption of another photon promotes the system to a higher excited state that could not be reached directly from the ground state. In this case, all previous experimental features encountered in the PL of silicon powder are correctly described: the zero initial slope and the time constants are linked to the existence of intermediate states, and the dependence on laser power is linked to the fact that the excited luminescent state is reached only when several photons are absorbed.

Systems showing a multistep-multiphoton excitation are often reported in the literature: excitation of rare-earth ions used as up photon converters[14] or transition-metal ions[15] in solid matrices. Since in those cases the energy levels of the system are revealed by the PL and optical-absorption spectra, a detailed study of the excitation dynamics is unnecessary. Our situation is radically different. As the PL spectra are unstructured, no direct information can be obtained about the energy levels. The exponent given by the dependence on laser power [Eq. (1)] would indicate at least a seven-step process for the luminescence at 1.55 eV, which is much higher than the usual two-step processes found in the literature. Moreover, this exponent depends on the spectral region (see Fig. 2). The situation is complicated, since the PL spectra fall at energies below the excitation photon (Fig. 1), whereas more energetic photons are usually emitted in processes of this kind.[14]

These findings cast doubt on the initial hypothesis that the PL emission in our samples is really a multistep-multiphoton process. A more detailed analysis of its excitation and deexcitation dynamics is necessary.

V. THEORY: DYNAMICS OF A MULTISTEP-MULTIPHOTON PROCESS

A schematic representation of the model to be analyzed is shown in Fig. 4. The system can be promoted to the m level by absorption of a photon when it is in the previous level $(m-1)$ in the chain. This process has a probability $\Phi\sigma_{m-1}$, where Φ is the excitation photon flux

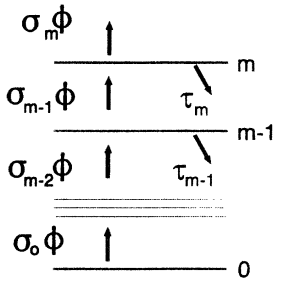

FIG. 4. Schematic representation of the multistep-multiphoton excitation process. An excited level can be reached only through the previous one.

and σ_{m-1} is the optical cross section. Once in the m level, it can be depopulated by deexcitation with the natural lifetime τ_m or by a photon absorption with probability $\sigma_m\Phi$. Both processes give an effective lifetime

$$\tau_m^{*-1}=\tau_m^{-1}+\sigma_m\phi \ , \tag{2}$$

which depends on the excitation flux. We suppose the deexcitation does not return the system to the previous level in the chain. This is a good simplification because the level population diminishes when its position is higher. Another reasonable approximation is to suppose that the system is far from saturation. That is, laser excitation does not appreciably change the population of the ground state.

This model can be described by the following set of differential equations:

$$\begin{aligned}
\frac{dn_1}{dt}&=\sigma_0\phi n_0-\frac{n_1}{\tau_1^*} \ , \\
\frac{dn_2}{dt}&=\sigma_1\phi n_1-\frac{n_2}{\tau_2^*} \ , \\
&\vdots \\
\frac{dn_m}{dt}&=\sigma_{m-1}\phi n_{m-1}-\frac{n_m}{\tau_m^*} \ ,
\end{aligned} \tag{3}$$

with the initial values depending on the excitation or deexcitation conditions. If m is the luminescent level, the PL intensity at any time will be proportional to $n_m(t)$. So its population can be monitored by the PL transient.

It is clear that for m greater than 2 the number of independent parameters is too large to allow a realistic fitting to the excitation transient. However, it is possible to obtain valuable information by analyzing some general properties of Eqs. (3).

A. Steady-state PL intensity

At the limit of $t \gg \tau_i^*$ all dependences on time vanish, and the population of the m level is

$$n_m(\infty)=n_0\prod_{i=1}^{m}\frac{\sigma_{i-1}\phi}{\sigma_i\phi+\tau_i^{-1}}=n_0\phi^m\prod_{i=1}^{m}\sigma_{i-1}\tau_i^* \ . \tag{4}$$

If $\tau_i^{-1} \gg \sigma_i\Phi$ (low laser excitation), the PL intensity is proportional to Φ^m. If $\sigma_i\Phi \gg \tau_i^{-1}$ for a particular level,

the exponent of Φ diminishes to $m-1$. So the exponent r in the experimental dependence of Eq. (1) gives a lower value for the position of the emitting level in the excitation chain.

B. Excitation dynamics

Equations (3) can be solved easily by hand. There are no mathematical difficulties in finding the time evolution for any arbitrary number of steps. Although the general solution can be given, it would be very cumbersome and would not give a clear image of the process. So, for clarity, we provide the more relevant features which can be proved by an inductive method.

The population of the mth level at any time can be written as

$$n_m(t)=n_m(\infty)+\sum_{i=1}^{m} A_i e^{-t/\tau_i^*} , \tag{5}$$

where $n_m(\infty)$ is the steady-state population, and A_i are constants that depend on the system parameters as well as on the excitation flux. The PL excitation transients at the limits of short and long times can now be easily analyzed by using formula (5) together with the differential Eqs. (3). The asymptotic behavior is very interesting because it provides simple methods to obtain useful information. It will be shown that at the limit of long times the PL transient gives the parameters τ_k and σ_k of the slowest level in the excitation chain. In addition, from the behavior at short times a lower value of m can be obtained.

1. Excitation transient at short times

From the differential equations it is easy to demonstrate that at $t=0$ the time derivatives of $n_m(t)$ are all zero until the mth order, which has the value

$$\left.\frac{d^m n_m}{dt^m}\right|_{t=0} = \phi^m n_0 \prod_{i=1}^{m} \sigma_{i-1} . \tag{6}$$

This means that at the limit of short times the behavior will be

$$n_m|_{t=0} = \left[\frac{1}{m!}\phi^m n_0 \prod_{i=1}^{m} \sigma_{i-1}\right] t^m . \tag{7}$$

This exponent can be obtained by a log-log plot of I_{PL} vs time of the excitation transient, provided that the time is short enough. By short enough, we mean that all exponentials in the general solution [Eq. (5)] can be approximated by their mth order in the Taylor expansion. That is, t smaller than the shortest τ_i^*. Of course, the experimental measurements are limited in time resolution. If one of the levels is faster than the time t_0 of the first acquisition ($\tau_j^* < t_0$), then it can be demonstrated that

$$n_m(t\to t_0) = \left[\frac{1}{(m-1)!}\Phi^m n_0 \tau_j^* \prod_{i=1}^{m} \sigma_{i-1}\right] t^{m-1} . \tag{8}$$

So, for a finite value of t_0, the effect in the measured transient of the faster levels will be a decrease in the exponent at short times:

$$I_{\mathrm{PL}}|_{t\to t_0} = A\phi^q t^s , \tag{9}$$

where s is just the number of levels slower than t_0. Thus it is a lower value of m. In addition, the exponent q that gives the dependence of the PL intensity on laser power at a given value of t tends to m as the laser power is low. As well as in the steady state [Eq. (4)], low laser power means $\Phi\sigma_j \gg \tau_j$; however, in this case this condition applies to states faster than t_0. It is instructive to remark that Eq. (8) is an intermediate expression between Eqs. (7) and (4), which are just the limit cases when t_0 tends to zero or to infinity, respectively.

2. Excitation transient at long times

It can be demonstrated that if the time constants are ordered as follows:

$$\tau_k^* > \tau_l^* > \cdots > \tau_m^* > \cdots , \tag{10}$$

then the constant linked to the slowest level, A_k, is negative, whereas the following one, A_l, is positive. This means that the transient at long times will be essentially monoexponential with a time constant τ_k^* which depends on Φ following Eq. (2). So the experimental transient can provide a measure of τ_k and σ_k corresponding to the slowest level.

C. PL transient decay

As in this experiment the laser excitation is held at zero, Eqs. (3) are no longer dependent. For the luminescent state, the decay of the PL will obey the equation

$$\frac{dn_m}{dt} = -\frac{n_m}{\tau_m} , \tag{11}$$

which means that, in contrast to the excitation, the decay transient will be exponential, with the decay time being the natural lifetime of the level:

$$I_{\mathrm{PL}}(t) = I(0)e^{-t/\tau_m} . \tag{12}$$

This agrees with the results reported in Sec. II. The decay time constant does not coincide with the excitation time constant because they correspond to different levels in the excitation chain: that is, the luminescent level and the slowest level in the chain, respectively.

D. Deexcitation dynamics of the intermediate states

While the population of the luminescent state can be monitored by the PL transient, information can be obtained about the population of the level just below the luminescent one. Imagine the experiment indicated in Fig. 5. After reaching the steady-state population the laser excitation is taken off during Δt. At this time every level will have a population

$$n_i(\Delta t) = n_{i\infty} e^{-\Delta t/\tau_i} . \tag{13}$$

These values are the initial conditions for the next excita-

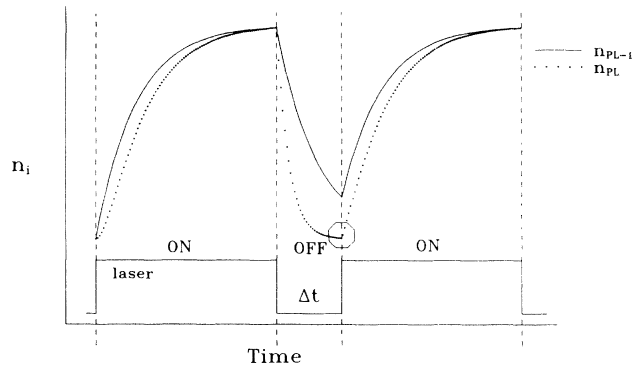

FIG. 5. Scheme showing the time evolution of the luminescent level population (dots) and its previous one (solid line). After reaching the steady state a decay is allowed during Δt, so that the previous level is not completely emptied. The following excitation transient begins with a finite slope.

tion transient. The most apparent effect will be the fact that now the slope at $t=0$ will be nonzero:

$$\left.\frac{dn_m}{dt}\right|_{t=0} = \phi\sigma_{m-1}n_{m-1}(\Delta t) - \frac{n_m(\Delta t)}{\tau_m^*} . \quad (14)$$

A clearer expression can be obtained by substituting (13) into (14) and making use of (4):

$$\left.\frac{dn_m}{dt}\right|_{t=0} = \frac{n_m(\infty)}{\tau_m^*}(e^{-\Delta t/\tau_{m-1}} - e^{-\Delta t/\tau_m}) . \quad (15)$$

So by measuring the slope at $t=0$ we can monitor the deexcitation dynamics of the level just below the luminescent one. Expression (15) gives two possibilities:

(a) $\tau_m < \tau_{m-1}$. In this case the excitation transient will always begin with a positive slope.

(b) $\tau_m > \tau_{m-1}$. Now the slope will always be negative.

In any case, the natural lifetime corresponding to the $m-1$ level can be obtained by fitting the transient obtained point by point by varying the deexcitation time delay.

VI. DETAILED MEASUREMENTS AND ANALYSIS

Now we are ready to analyze more detailed measurements that have been performed in order to verify that, indeed, the multistep-multiphoton process is governing the PL observed in our samples. In addition, the model offers us the possibility to evaluate some important physical parameters such as the optical capture cross section. Unless stated otherwise, all experiments were carried out by integrating the PL spectra from 0.7 to 0.4 eV. In this region, the interpretation of the results is simpler than at 1.55 eV. This is not surprising in view of the dependence on laser power. At 1.55 eV, seven steps are necessary to account for this dependence, whereas we need only three steps in the 0.7–0.4-eV region.

In order to highlight the very good agreement with the predictions of the model described in Sec. V, we follow a similar structure in the exposition. So the reader is invited to read this section with frequent glances to the previous one.

A. Excitation transient at short times

Until now, the main indication that there are many steps involved in the PL of silicon powder has come from the dependence of the PL intensity on laser power at the steady state (Fig. 2). The analysis of the PL excitation transients affords an additional quantification of the number of steps. In addition, the results show a clear internal consistency.

In Fig. 6 the excitation transients corresponding to the PL emission in the 0.4–0.7-eV region for different laser powers are shown in a log-log plot. The time of the first acquisition, t_0, is about 10 ms. The main experimental limitation to detailing the transient for shorter times is the signal itself: as its first derivatives are zero, the signal is very small for short times. As seen in Fig. 6, the slope is nearly 3, indicating that $m \geq s = 3$ [Eq. (9)]. That is, the luminescent level emitting at 0.7–0.4 eV is, at least, the third level in the excitation chain. The same conclusion is reached by plotting the intensity at 20 ms vs laser power according to Eq. (9) (Fig. 8).

Similar measurements have been carried out with the luminescence at 1.55 eV (Fig. 7). The slope at short times is about 2 ($s=2$). In this case, this is a value much shorter than that obtained in Fig. 8, where we obtain $q=7$. In view of formula (8), this result means that the emission at 1.55 eV corresponds to at least the seventh level in the chain ($m \geq q=7$). Moreover, from the difference $q-s=5$, we deduce that five of the levels do not contribute to the transients for times longer than 2 ms (Fig. 7), which means that their lifetimes are shorter.

Another feature to be analyzed is the fact that the dependence of PL intensity on laser power is not the same at the steady state (Fig. 2) or at the limit of short

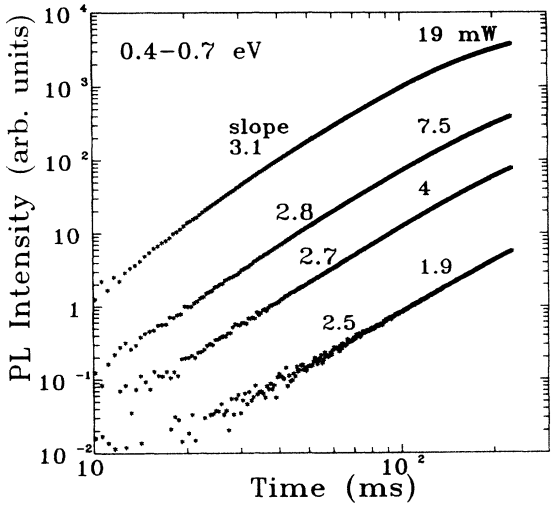

FIG. 6. The beginning of excitation transients. The PL intensity has been integrated between 0.4 and 0.7 eV. The slope is related to the steps needed to reach the luminescent level.

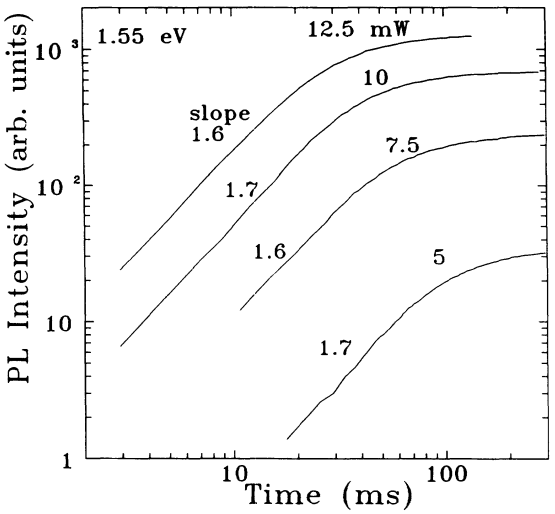

FIG. 7. As for Fig. 6 but for an emitted photon energy of 1.55 eV.

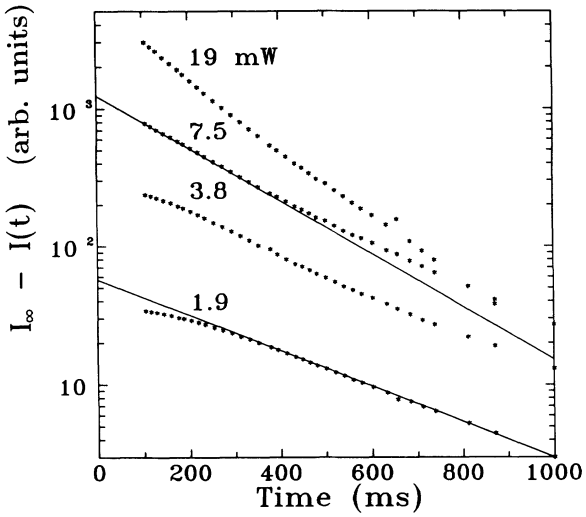

FIG. 9. Excitation transients at the 0.4–0.7-eV spectral range. Note that the transients become more exponential with lower laser powers.

times (Fig. 8). By comparing these figures we can clearly see that, at short times, the dependence given by Eq. (1) is better followed. This can be easily understood within our model. The experimental points in the two figures do not exactly match Eq. (1) due to the evolution of the effective lifetime with excitation power [Eq. (2)]. This effect is less pronounced in the PL intensity at short times because only lifetimes faster than t_0 contribute to Eq. (8), whereas all are contributing in the steady-state intensity [Eq. (4)].

B. Excitation transients at long times

As demonstrated in the corresponding section (V B 2), the behavior of the excitation transient at the limit of long times is basically exponential and is related to the slowest level parameters.

In Fig. 9 the excitation transients measured at laser powers ranging from 1.9 to 19 mW are shown. It is clear that as the excitation flux becomes smaller the transient becomes slower and more exponential. Both features can be easily interpreted within our model framework.

At long times, the excitation transient must be monoexponential with the effective lifetime of the slowest level in the chain. According to Eq. (2) the effective lifetime depends on the excitation photon flux. This explains why the transients are quicker at higher powers. The nonexponentiality is due to a nonuniformity in the excitation flux. As the laser beam penetrates into the sample its intensity is reduced monotonically due to optical absorption. So the effective lifetime depends on the distance of the emitting point from the sample surface, and the transient is nonexponential. As the laser power diminishes the effective lifetime tends to the natural lifetime [Eq. (2)]. So at this limit the time constant is the natural lifetime of the level.

The transient slopes have been plotted against Φ in Fig. 10. Following Eq. (2), this leads to the evaluation of the level parameters corresponding to the slowest level. The natural lifetime is $\tau = 420 \pm 50$ ms, and the optical capture cross section is $\sigma = 3 \times 10^{-18}$ cm^2. The error bars in those values come basically from the nonexponential behavior already described.

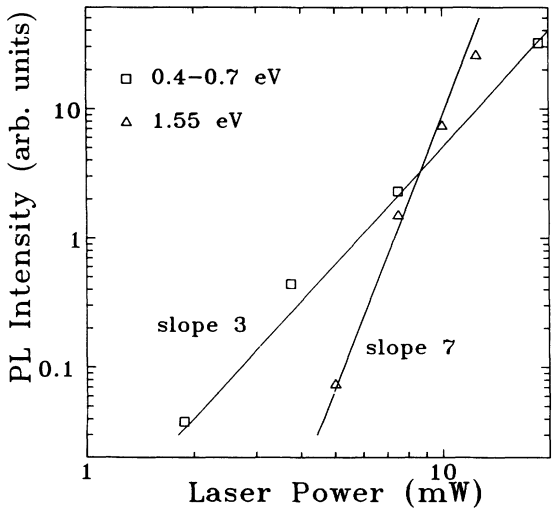

FIG. 8. PL intensity at 20 ms after the beginning of the excitation pulse obtained from Figs. 6 and 7. Note that the dependence on laser power is more linear than at the steady state (Fig. 1).

C. Deexcitation transient

Remember that, following Eq. (12), the PL decay is governed by the natural lifetime of the luminescent level.

The PL decay transients show a clear nonexponential behavior (Fig. 11). At 19 mW, the slope at $t=0$ gives a lower limit of the time constants contributing to the transient of 8 ms, which is increased to 55 ms at 1.2 mW, indicating that the transient becomes slower. At long times

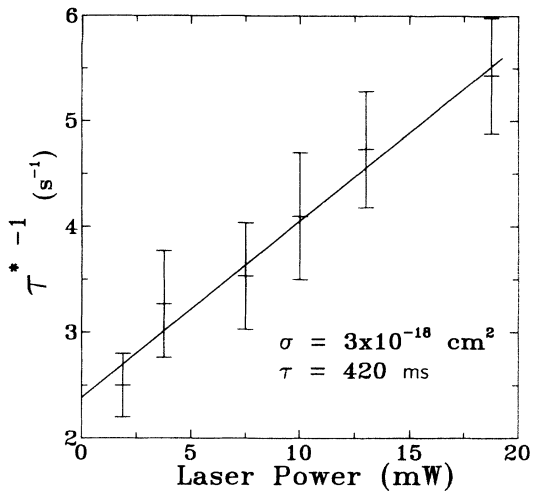

FIG. 10. Effective lifetime obtained from Fig. 9. The slope is proportional to the optical cross section of the slowest level in the excitation chain.

a common time constant for all powers of 125 ms is obtained. Nevertheless, this value is more inaccurate due to the difficulty in setting the signal properly at $t \rightarrow \infty$. To avoid this problem of baseline, a good method is to take the time derivative of the transient as follows.

Let us assume that the transient has its origin in a superposition of different time constants described by the distribution $D(\tau)$:

$$I(t)=\int_0^{\infty} D(\tau)e^{-t/\tau}d\tau \ . \tag{16}$$

Derivation of Eq. (16) gives

$$\frac{dI(t)}{d\ln t}=\int_{-\infty}^{+\infty} F(\tau)e^{-\exp(\theta_t-\theta_\tau)}\exp(\theta_t-\theta_\tau)d\tau$$

$$\equiv F\otimes P_{\mathrm{ICTS}} \ , \tag{17}$$

where the sign $\otimes$ means the convolution product and P_{ICTS} is the peak we would obtain with a monoexponential transient, and the following substitution has been introduced:

$$\theta_t=\ln t, \quad \theta_\tau=\ln\tau \ . \tag{18}$$

The function

$$F(\tau)=D(\tau)\frac{d\tau}{d\ln\tau}=\tau D(\tau) \tag{19}$$

is the distribution of time constants in a log scale. Equation (17) tells us that the logarithmic derivative of the transient is just the time constant distribution convoluted by the ICTS peak (solid line in Fig. 12). This kind of analysis comes from the experimental characterization of deep levels by capacitance techniques,[16] so ICTS means isothermal transient capacitance spectroscopy. A similar result is obtained in Ref. 17, where it is concluded that when $F(\tau)$ is broad enough it coincides with the time derivative. In Fig. 12 we see that the ICTS peak FWHM (full width at half maximum) is 1.1 decades broad, giving a quantification of the resolution achieved by this technique.

The normalized time derivatives of the transient at several power excitations are shown in Fig. 12. The result is a curve that is too narrow to be identified with the time constant distribution, $F(\tau)$. Taking $F(\tau)$ as the Gaussian distributions of Fig. 13, a good fit is obtained. The parameters describing $F(\tau)$ are summarized in Table I. There is a clear evolution: as the laser power decreases, the distribution becomes narrower and shifts to longer times.

The fact that the deexcitation transient is not monoexponential is easily integrated in the model by allowing a broadening in the luminescent level into a subset of closely spaced sublevels. What is less clear is the evolution with the excitation power. It could be due to a depen-

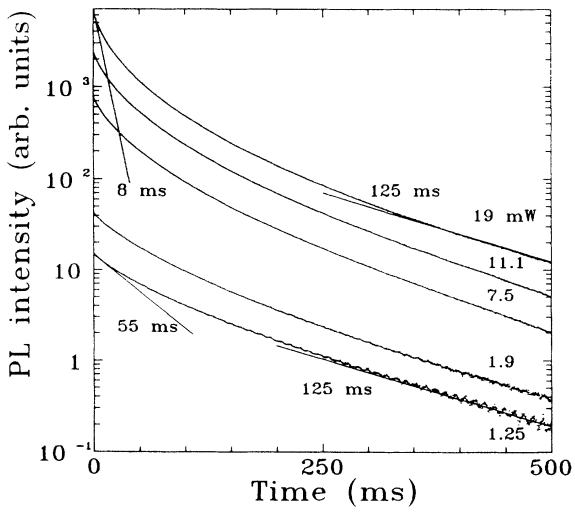

FIG. 11. PL decay transients at the 0.4–0.7 spectral range.

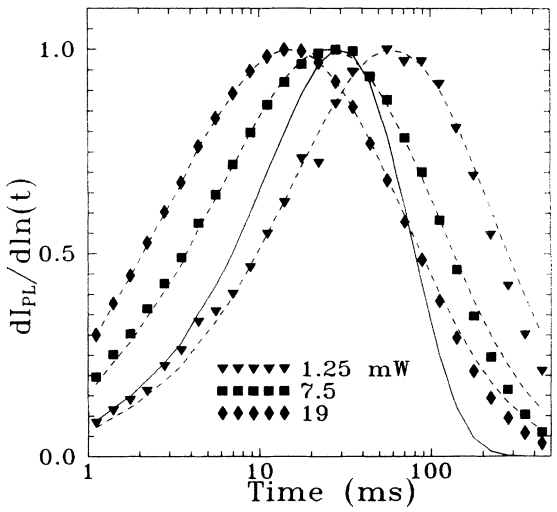

FIG. 12. Time derivatives of several transients of Fig. 11 (points) with fittings obtained by supposing the Gaussian distributions of time constants of Fig. 13 (broken lines). For comparison, the solid line corresponds to an exponential transient.

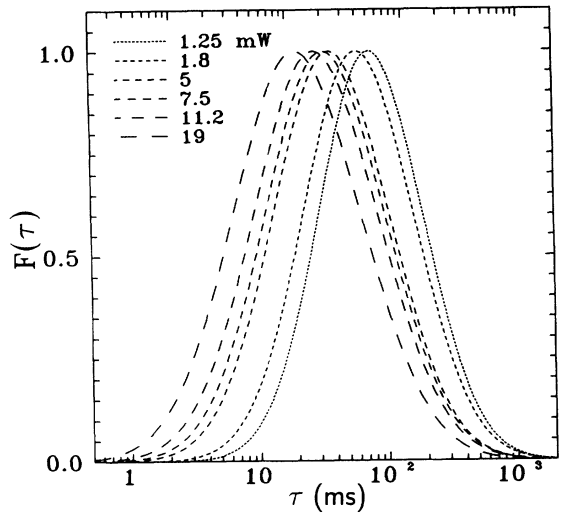

FIG. 13. Time constant distributions of the PL decay transients.

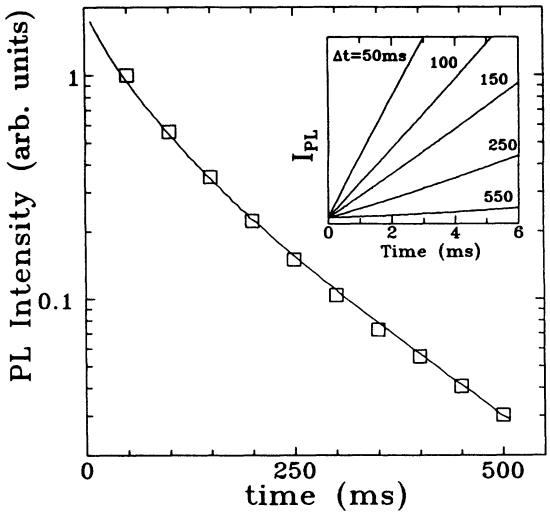

FIG. 14. Slope at $t=0$ after a deexcitation lasting Δt (triangles). The curve is just the PL decay transient at 1.2 mW of Fig. 11. The inset shows the beginning of the excitation transient.

dence on power of the population in the sublevels corresponding to a saturation of the lowest-lying ones. Alternatively, the contribution of two levels of the excitation scheme (say m and $m-1$) to the PL spectrum can be considered. In this case, as the relative contribution of the highest level increases with excitation power, this level should be quicker than the previous one to account for the experimental evolution of $F(\tau)$. Although not definitive, the results described in Sec. VI D afford proof of the second possibility. That is, more than one level contributes to the PL emission.

D. Deexcitation dynamics of the intermediate states

The experiment proposed in Fig. 5 has been performed with an excitation time of 4 s, which ensures that the system reaches the steady state. Afterwards, deexcitation is allowed during a delay Δt varying from 50 to 800 ms, before another excitation begins. As expected from the model, the slope at the beginning of the excitation transient is now nonzero (Fig. 14). This occurs even with $\Delta t=800$ ms. That is, after the PL decay is finished. Therefore, at this delay, at least one intermediate state is still populated. We think that this is a definitive proof of the existence of intermediate levels, which confirms that the model proposed is appropriate to describe our results.

TABLE I. Standard deviation (σ) and mean time constant (τ_0) describing the distribution $F(\tau)$ at different excitation powers.

Excitation power (mW)	σ (decades)	τ_0 (ms)
1.2	0.93	75
1.9	0.97	60
5	1.03	37
7.5	1.07	33
11	1.10	28
19	1.15	20

The slope has been plotted vs the delay time in Fig. 14. We can obtain useful information if we analyze it in view of Eq. (15). First, as the slope is positive we can conclude that the level below the luminescent one has a longer lifetime. In fact, the points in Fig. 14 give its depopulation transient. The measurements have been made with a laser power of 12 mW. At these conditions the PL decays with a mean time constant of 28 ms (Table I). This means that, as the shortest delay is 50 ms, the luminescent level does not contribute to the slope because after the delay it is almost completely depopulated. So the points in Fig. 14 give the depopulation transient of the previous level in the chain directly. We see that it has nonexponential dynamics, with a mean lifetime between that of the luminescent level ($\tau=28$ ms) and the slowest lifetime in the chain ($\tau=420$ ms).

What is really surprising is the coincidence between the depopulation transient and the PL decay measured at 1.2 mW (solid curve in Fig. 14). This indicates that we are monitoring the depopulation of the $m-1$ level (the level previous to the main luminescent one) in two ways. This constitutes a proof that the $m-1$ level also contributes to the PL. As pointed out in Sec. VI C, more than one level contributes to the PL spectra, their relative contribution depending on the laser power.

VII. SUMMARY AND DISCUSSION

At this point, we are very pleased to note that most of the features found in the experimental transients can be understood within the multistep-multiphoton model. The quantitative analysis has delivered detailed information concerning the levels involved in the observed PL. A summary follows.

In the 0.4–0.7-eV range, the PL comes mainly from a level located in at least the third step ($m=3$) in the excitation chain. In fact, the results do not indicate a higher

position. Its lifetime is $\tau_3 \approx 20$ ms. The previous level is thought to contribute appreciably to the PL emission at low excitation powers, its lifetime being $\tau_2 \approx 70$ ms. Below this, the slowest level is found to have a very long lifetime $\tau_1 \approx 400$ ms. In addition, its optical cross section is $\sigma_1 = 3 \times 10^{-18}$ cm^2. The second and third levels show nonexponential dynamics, indicating a sublevel structure. The 1.55-eV emission comes from at least the seventh level in the excitation chain. Although its dynamics has not been studied it detail, it gives useful information concerning the PL spectra: the structureless broad PL band receives contributions from many levels.

The most puzzling feature is the energy of the emitted photons. In a multiphoton process, the emitted photon is usually more energetic than the excitation one. This is so because the main reason why the PL level cannot be reached directly from the ground state is its high energy. In our case, to collect a photon of 0.5 eV, three steps (that is, an energy of $3 \times 2.5 = 7.5$ eV) are needed. Apparently the luminescent state is not so energetic and presumably its energy is lower than the excitation photon. So the questions arise as to what prevents direct excitation from the ground state, and how the excess energy is relaxed.

Although remaining inside a very formal level of comprehension, the model designed in Fig. 15 fulfills all requirements. Every level in the excitation scheme of Fig. 4 is just the ground state of the quantum wells of Fig. 15. In this model, excitation and deexcitation are only possible between neighboring wells because the potential barriers limit the spread of the wave functions around the well. After absorption of one photon, the excess energy is relaxed nonradiatively with a very short time constant (τ_{nr}). Once in the ground state of the well, photon emission is needed to return to the previous well with a much slower time constant (τ_r). In the case where $\tau_{nr} \ll \tau_r$, the dynamics of this model will be correctly described by Eqs. (3). The feeding of the levels by the deexcitation of the higher ones can be ignored if the population diminishes enough with increasing level position.

The multistep-multiphoton process sketched in Fig. 4 has been demonstrated to account for all experimental facts related to PL dynamics, and future experiments will have to be interpreted into this framework. However, the more detailed model of Fig. 15, that has been proposed to account mainly for the low energy of the emitted photon, is very speculative and its physical implementation remains an open question. The wells cannot be the usual

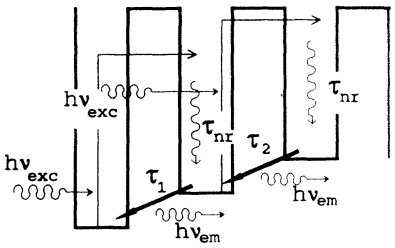

FIG. 15. Schematic representation of a somewhat more refined model to explain why the system can be excited only step by step, and why the emitted photon is always less energetic than the excitation photon. After absorption of a photon the system relaxes nonradiatively with a lifetime of τ_{nr} much shorter than the level lifetime (τ_i).

wells that are built into the conduction and valence bands in semiconductors. If this were the case, the electron-hole pair created by the exciting photon would recombine before any migration to the neighboring wells. A possible physical implementation of this model could be a set of excited electron states with a strong electron-phonon coupling. In this case, the wells will be the parabolas of the adiabatic potential, widely used in point-defect theory,[18] placed not in the real space but in the space of the configuration coordinate.

To elucidate the microscopical significance of the proposed model and, consequently, the physical origin of the observed PL, further studies are under way. What is clear is the fact we are faced with a PL emission which has no counterparts in the Si-powder-related materials. The measured PL decay and excitation lifetimes are about four orders of magnitude longer than the longest lifetimes reported for porous silicon.[19–21] Those long lifetimes support the idea of tunnel-like optical transitions contained in the model of Fig. 15. Moreover, a small deformation given by an external pressure could modify the wave function overlap and, consequently, the PL intensity. Indeed, this dependence on pressure together with the multistep-muliphoton emission are the fingerprints of the PL emission observed in PECVD silicon powders.

ACKNOWLEDGMENT

This work was partially supported by the C.E.C. BRITE-EURAM Program under Contract No. BRE2-CT94-0944.

[1]Proceedings of the 39th National Symposium of the American Vacuum Society, Part II [J. Vac. Sci. Technol. A **11** (4) (1994)].

[2]Proceedings of the NATO Advanced Research Workshop: Formation, Transport and Consequences of Particles in Plasmas [Plasma Sources Sci. Technol. **3**, 239 (1994)].

[3]L. T. Canham, Appl. Phys. Lett. **57**, 1046 (1990).

[4]S. Furukawa and T. Hiyasato, Phys. Rev. B **36**, 5726 (1988).

[5]Ch. Hollenstein, J.-L. Dorier, J. Dutta, and A. A. Howling, Plasma Sources Sci. Technol. **3**, 278 (1994).

[6]J. Costa, P. Roura, G. Sardin, J. R. Morante, and E. Bertran, Appl. Phys. Lett. **64**, 463 (1994).

[7]J. Costa, P. Roura, G. Sardin, J. R. Morante, and E. Bertran, in *Molecularly Designed Ultrafine/Nanostructured Materials*, edited by K. E. Gonsalves, G.-M. Chow, T. D. Xiao, and R. C. Cammarata, MRS Symposia Proceedings No. 351 (Materials Research Society, Pittsburgh, 1994), pp. 405–410.

[8]J. Costa, G. Sardin, J. Campmany, and E. Bertran, Vacuum **45**, 1115 (1994).

[9]E. Bertran, J. Costa, G. Sardin, J. Campmany, J. Landujar, and

A. Canillas, Plasma Sources Sci. Technol. **3**, 348 (1994); J. Costa, G. Sardin, J. Campmany, J. Landujar, A. Canillas, and E. Bertran, in *Amorphous Silicon Technology—1993,* edited by E. A. Schiff, M. J. Thompson, A. Madan, K. Tanaka, and P. G. LeComber, MRS Symposia Proceedings No. 297 (Materials Research Society, Pittsburgh, 1993), p. 1031.

[10]G. Armagan, B. Di Bartolo, and A. M. Buoncristiani, J. Lumin. **44**, 129 (1989).

[11]E. Chimczak, Z. Phys. B **72**, 211 (1988).

[12]E. Chimczak, W. S. Gordon, and M. Bertrand-Zytkowiak, Phys. Status Solidi A **82**, 527 (1984).

[13]R. R. Birge, Acc. Chem. Res. **19**, 138 (1986).

[14]X. Wu, J. P. Denis, G. Özen, Ph. Goldner, M. Genotelle, and F. Pellé, Chem. Phys. Lett. **203**, 211 (1993).

[15]U. Oetliker, M. J. Riley, P. S. May, and H. U. Güdel, J. Lumin. **53**, 553 (1992).

[16]H. Okushi and Y. Tokumaru, Jpn. J. Appl. Phys. **19**, L335 (1980).

[17]C. Tsang and R. A. Street, Phys. Rev. B **19**, 3027 (1979).

[18]K. K. Rebane, *Impurity Spectra of Solids* (Plenum, New York, 1970).

[19]T. P. Pearsall, J. C. Adams, J. E. Wu, B. Z. Nosho, Ch. Aw, and J. C. Patton, J. Appl. Phys. **71**, 4470 (1992).

[20]L. R. Tessler, F. Alvarez, and O. Teschke, Appl. Phys. Lett. **62**, 2381 (1993).

[21]K. Wang, D. Han, M. Kemp, and M. Silver, Appl. Phys. Lett. **62**, 157 (1992).